J|A|C|S
ARTICLES
Published on Web 01/13/2007

X-ray Absorption and EPR Spectroscopic Studies of the Biotransformations of Chromium(VI) in Mammalian Cells. Is Chromodulin an Artifact of Isolation Methods?

Aviva Levina, Hugh H. Harris, and Peter A. Lay*

Contribution from the Centre for Heavy Metals Research, and Centre for Structural Biology and Structural Chemistry, School of Chemistry, The University of Sydney, NSW, 2006, Australia

Received June 9, 2006; E-mail: p.lay@chem.usyd.edu.au

Abstract: Very different biological activities are usually ascribed to Cr(VI) (a toxin and carcinogen) and Cr(III) (an antidiabetic agent), although recent evidence suggests that both these types of actions are likely to arise from cellular uptake of varying concentrations of Cr(VI). The first systematic study of XANES spectra of Cr(III) complexes formed in Cr(VI)-treated mammalian cells (A549, HepG2, V79, and C2C12 cell lines), and in subcellular fractions of A549 cells, has been performed using a library of XANES spectra of model Cr(III) complexes. The results of multiple linear regression analyses of XANES spectra, in combination with multiple-scattering fits of XAFS spectra, indicate that Cr(III) formed in Cr(VI)-treated cells is most likely to bind to carboxylato, amine, and imidazole residues of amino acids, and to a lesser extent to hydroxo or aqua ligands. A combination of XANES and EPR spectroscopic data for Cr(VI)-treated cells indicates that the main component of Cr(III) formed in such cells is bound to high-molecular-mass ligands (>30 kDa, probably proteins), but significant redistribution of Cr(III) occurs during the cell lysis, which leads to the formation of a low-molecular-mass (<30 kDa) Cr(III)-containing fraction. The spectroscopic (XANES, XAFS, and EPR) properties of this fraction were strikingly similar to those of the purported natural Cr(III)-containing factor, chromodulin, that was reported to be isolated from the reaction of Cr(VI) with liver. These data support the hypothesis that a chromodulin-like species, which is formed from such a reaction, is an artifact of the reported isolation procedure.

Introduction

Two very different types of biological activities are usually ascribed to Cr compounds, including well-established cytotoxicity, genotoxicity, and carcinogenicity of Cr(VI)[1−3] and a controversial role of Cr(III) as an essential micronutrient involved in insulin-dependent glucose metabolism.[4−7] The high toxicity of Cr(VI) is based on the active transport of $[CrO_4]^{2-}$ (isostructural with $[SO_4]^{2-}$ and $[HPO_4]^{2-}$) into cells, followed by its reactions with cellular reductants (such as glutathione, ascorbate, or NAD(P)H-dependent enzymes).[2,8] Such reactions produce highly reactive intermediates, including Cr(V/IV) complexes and organic radicals, and ultimately lead to the formation of stable (kinetically inert) Cr(III) complexes with biological ligands, including genotoxic Cr(III)−DNA adducts.[2,8,9,10] By contrast, the suggested role of Cr(III) in insulin potentiation is difficult to explain from the chemical point of view, given the kinetic inertness of Cr(III) complexes and their inability to enter cells at significant rates.[2,6,7] A mechanism based on the selective activation of insulin receptor tyrosine kinase by a specific Cr(III)-containing biomolecule, chromodulin, has been proposed.[4] Chromodulin, believed to be a tetranuclear Cr(III) assembly bound to a small peptide ligand, has not been fully characterized to date.[11] Several researchers have questioned the existence of chromodulin,[2,12] based on the reported method of its isolation (reactions of high concentrations of exogenous Cr(VI) with bovine liver homogenate).[13]

Recently, we have proposed an alternative explanation for the insulin-potentiating activity of Cr(III) complexes, based on their extra- and/or intracellular oxidation to Cr(VI) by biological oxidants, such as H_2O_2 or ClO^-.[14−16] The resultant Cr(VI) can

(1) International Agency for Research on Cancer. *Overall Evaluations of Carcinogenicity to Humans*; Lyon, France, 2003.
(2) Levina, A.; Codd, R.; Dillon, C. T.; Lay, P. A. *Prog. Inorg. Chem.* **2003**, *51*, 145−240, and references therein.
(3) Guertin, J. In *Chromium(VI) Handbook*; Guertin, J.; Jacobs, J. A.; Avakian, C. P., Eds.; CRC Press: Boca Raton, FL, 2005; pp 215−234.
(4) Vincent, J. B. *Polyhedron* **2001**, *20*, 1−26.
(5) Cefalu, W. T.; Hu, F. B. *Diabetes Care* **2004**, *27*, 2741−2751.
(6) Stearns, D. M. *BioFactors* **2000**, *11*, 149−162.
(7) Martin, R. B. In *Handbook on metalloproteins*; Bertini, I.; Sigel, A.; Sigel, H., Eds.; Marcel Dekker: New York, 2001; pp 181−192.
(8) Connett, P.; Wetterhahn, K. E. *Struct. Bonding (Berlin)* **1983**, *54*, 93−124.
(9) Zhitkovich, A. *Chem. Res. Toxicol.* **2005**, *18*, 3−11.
(10) O'Brien, T. J.; Ceryak, S.; Patierno, S. R. *Mutat. Res.* **2003**, *533*, 3−36.
(11) Jacquamet, L.; Sun, Y. J.; Hatfield, J.; Gu, W. W.; Cramer, S. P.; Crowder, M. W.; Lorigan, G. A.; Vincent, J. B.; Latour, J. M. *J. Am. Chem. Soc.* **2003**, *125*, 774−780.
(12) Gaggelli, E.; Berti, F.; D'Amelio, N.; Gaggelli, N.; Valensin, G.; Bovalini, L.; Paffetti, A.; Trabalzini, L. *Environ. Health. Persp. Suppl. 5.* **2002**, *110*, 733−738.
(13) Davis, C. M.; Vincent, J. B. *Arch. Biochem. Biophys.* **1997**, *339*, 335−343.
(14) Mulyani, I.; Levina, A.; Lay, P. A. *Angew. Chem., Int. Ed. Engl.* **2004**, *43*, 4504−4507.
(15) Levina, A.; Mulyani, I.; Lay, P. A. In *New Advances in the Biochemistry of Chromium(III)*; Vincent, J. B., Ed.; Elsevier Science: New York (in press).
(16) Wu, L. E.; Levina, A.; Harris, H. H.; Cai, Z.; Lai, B.; Vogt, S.; James, D. E.; Lay, P. A. To be submitted.

act as a tyrosine phosphatase inhibitor, similar to the isoelectronic V(V) (which is a well-known insulin-mimetic and an antidiabetic agent).[17] The presence of Cr(VI) will also lead to increased glucose metabolism due to oxidative stress. Small amounts of Cr(VI), formed by the relatively slow oxidation of Cr(III), are likely to be reduced within the cellular membrane or in the cytoplasm, prior to reaching the nucleus.[15,18] The main effects of Cr(VI) in this case are likely to be alterations in cell signaling,[19] including insulin potentiation due to the inhibition of tyrosine phosphatases involved in the insulin signaling cascade.[14,15,20] Exposure of cells to higher concentrations of exogenous Cr(VI) will overwhelm the cellular protective mechanisms and lead to accumulation of Cr(III)−DNA adducts in the nucleus,[15,18,21] which is believed to be the main cause of Cr(VI)-induced cytotoxicity and genotoxicity.[9,10] Thus, understanding of both beneficial and harmful effects of Cr compounds requires a knowledge of chemical mechanisms of Cr(VI) reactions with cellular components and the nature of Cr(III) products formed in such reactions. Our approach to this problem is the use of a combination of synchrotron-based techniques, including X-ray fluorescence (XRF) elemental mapping of single cells, microprobe X-ray absorption near-edge structure (XANES) spectroscopy of Cr hotspots in single cells, and XANES and X-ray absorption fine structure (XAFS) spectroscopy of bulk samples of Cr-treated cells.[18,21,22] In addition, electron paramagnetic resonance (EPR) spectroscopy is used for selective detection and characterization of Cr(V) intermediates formed during the biological reduction of Cr(VI).[2]

In recent years, XANES spectroscopy has developed into a powerful tool for the study of chemical speciation of metal ions in biological and environmental samples. It has the ability to probe specific spectroscopic signatures of metal ions, regardless of the physical state and chemical composition of the sample.[23] The abilities of XANES spectroscopy to detect low (micromolar) concentrations of metal ions, and its high sensitivity to small changes in the coordination environments of metal ions, make it particularly useful for biological samples (in comparison with a related technique, XAFS spectroscopy).[23−26] Despite some developments in theory,[27−29] no readily available computational tools exist to date for accurate prediction of coordination environments of metal ions from their XANES spectra (unlike for the more theoretically advanced XAFS spectroscopy).[30] For this reason, empirical methods based on comparison of studied XANES spectra with those of known model compounds are widely used; these include principal component, target transformation, and multiple linear regression analyses.[25,26,31,32]

Previous XANES spectroscopic studies of biological samples have focused mainly on changes in the oxidation states of metal ions in cells and tissues.[33−35] In particular, numerous observations of efficient reductions of Cr(VI) to Cr(III) in biological media were based on the disappearance of the characteristic preedge absorbance peak of Cr(VI) in XANES spectra.[18,21,22,36−39] Fewer studies have attempted to assign the coordination environments of the Cr(III) products of Cr(VI) reductions,[38,39] and these assignments have been based on a limited number of model compounds, which were often poorly characterized (e.g., commercial Cr(III) acetate, known to contain varying amounts of trimeric, octameric, and polymeric species).[40] This work is the first to use an extensive library of model Cr(III) compounds to characterize the chemical forms of Cr in mammalian cells treated with Cr(VI) by XANES spectroscopy (in combination with XAFS and EPR techniques). Apart from providing insights into the metabolism of carcinogenic Cr(VI), the research is also aimed at testing whether the intracellular product of the reaction of Cr(VI) with liver cells is chromodulin or whether this is an artifact of the isolation procedure.

Experimental Section

Caution. Chromium(VI) compounds are human carcinogens;[1] skin contact and inhalation must be avoided.

Materials. Analytical or higher grade reagents were purchased from Merck or Sigma-Aldrich and were used without further purifications. Water was purified by the MilliQ technique. Presterilized solutions and sterile disposable plasticware, used in cell culture work, were purchased from Gibco and Becton Dickinson, respectively. Model Cr(III) complexes (**A1**−**A17** in Table 1) were synthesized by literature procedures (some with modifications),[40−59] and their purities were confirmed by

(17) Thompson, K. H.; Orvig, C. In *Metal Ions in Biological Systems*; Siegel, A.; Siegel, H., Eds.; Marcel Dekker: New York, 2004; Vol 41 (Metal Ions and their Complexes in Medication), pp 221−252.
(18) Harris, H. H.; Levina, A.; Dillon, C. T.; Mulyani, I.; Lai, B.; Cai, Z.; Lay, P. A. *J. Biol. Inorg. Chem.* **2005**, *10*, 105−118.
(19) Barchowsky, A.; O'Hara, K. A. *Free Rad. Biol. Med.* **2003**, *34*, 1130−1135.
(20) Yurkow, E. J.; Kim, G. *Mol. Pharmacol.* **1995**, *47*, 686−695.
(21) Dillon, C. T.; Lay, P. A.; Kennedy, B. J.; Stampfl, A. P. J.; Cai, Z.; Ilinski, P.; Rodrigues, W.; Legnini, D.; Lai, B.; Maser, J. *J. Biol. Inorg. Chem.* **2002**, *7*, 640−645.
(22) Dillon, C. T.; Lay, P. A.; Cholewa, M.; Legge, G. J. F.; Bonin, A. M.; Collins, T. J.; Kostka, K. L.; Shea-McCarthy, G. *Chem. Res. Toxicol.* **1997**, *10*, 533−535.
(23) Gunter, K. K.; Miller, L. M.; Aschner, M.; Eliseev, R.; Depuis, D.; Gavin, C. E.; Gunter, T. E. *Neurotoxicology* **2002**, *23*, 127−146.
(24) Harris, H. H.; Pickering, I. J.; George, G. N. *Science* **2003**, *301*, 1203−1204.
(25) Pickering, I. J.; Prince, R. C.; Salt, D. E.; George, G. N. *Proc. Natl. Acad. Sci. U.S.A.* **2000**, *97*, 10717−10722.
(26) Frank, P.; Carlson, R. M. K.; Carlson, E. J.; Hodgson, K. O. *Coord. Chem. Rev.* **2003**, *237*, 31−39.
(27) Rehr, J. J.; Ankudinov, A. L. *Coord. Chem. Rev.* **2005**, *249*, 131−140.
(28) Boffi, F.; Ascone, I.; Della Longa, S.; Girasole, M.; Yalovega, G.; Soldatov, A. V.; Varoli-Piazza. A.; Congiu Castellano, A. *Eur. Biophys. J.* **2003**, *32*, 329−341.
(29) Pantelouris, A.; Modrow, H.; Pantelouris, M.; Hormes, J.; Reinen, D. *Chem. Phys.* **2004**, *300*, 13−22.
(30) Levina, A.; Armstrong, R. S.; Lay, P. A. *Coord. Chem. Rev.* **2005**, *249*, 141−160.
(31) Ressler, T.; Wong, J.; Roos, J.; Smith, I. L. *Environ. Sci. Technol.* **2000**, *34*, 950−958.
(32) Beauchemin, S.; Hesterberg, D.; Beauchemin, M. *Soil Sci. Soc. Am. J.* **2002**, *66*, 83−91.
(33) Hall, M. D.; Foran, G. J.; Zhang, M.; Beale, P. J.; Hambley, T. W. *J. Am. Chem. Soc.* **2003**, *125*, 7524−7525.
(34) Ide-Ektessabi, A.; Kawakami, T.; Watt, F. *Nucl. Instr. Met. Phys. Res. B* **2004**, *213*, 590−594.
(35) Gunter, T. E.; Miller, L. M.; Gavin, C. E.; Eliseev, R.; Salter, J.; Buntinas, L.; Alexandrov, A.; Hammond, S.; Gunter, K. K. *J. Neurochem.* **2004**, *88*, 266−280.
(36) Ortega, R.; Fayard, B.; Salomé, M.; Devès, G.; Susini, J. *Chem. Res. Toxicol.* **2005**, *18*, 1512−1519.
(37) Kemner, K. M.; Kelly, S. D.; Lai, B.; Maser, J.; O'Loughlin, E. J.; Sholto-Douglas, D.; Cai, Z.; Schneegurt, M. A.; Kulpa, C. F.; Nealson, K. H. *Science* **2004**, *306*, 686−687.
(38) Hu, M.-J.; Wei, Y.-L.; Yang, Y.-W.; Lee, J.-F. *J. Phys. Condens. Matter.* **2004**, S3473−S3478.
(39) Bluskov, S.; Arocena, J. M.; Omotoso, O. O.; Young, J. P. *Int. J. Phytoremed.* **2005**, *7*, 153−165.
(40) Eshel, M.; Bino, A. *Inorg. Chim. Acta* **2001**, *320*, 127−132.
(41) Lazar, D.; Ribár, B.; Divjakovič, V.; Mészáros, C. *Acta. Crystallogr.* **1991**, *C47*, 1060−1062.
(42) Hinz, D. *Z. Anorg. Allg. Chem.* **2000**, *626*, 1004−1011.
(43) *Handbook of preparative inorganic chemistry* 2nd ed.; Brauer, G. Ed.; Academic Press: New York, 1965; Vol. 2, pp 1354−1355.
(44) *Handbook of preparative inorganic chemistry*, 2nd ed.; Brauer, G. Ed.; Academic Press: New York, 1965; Vol. 2, pp 1372−1373.
(45) Isied, S. S.; Kuo, G.; Raymond, K. N. *J. Am. Chem. Soc.* **1976**, *98*, 1763−1767.
(46) Levina, A.; Foran, G. J.; Pattison, D. I.; Lay, P. A. *Angew. Chem., Int. Ed.* **2004**, *43*, 462−465.
(47) Raston, C. L.; White, A. H. *Aust. J. Chem.* **1977**, *30*, 2091−2094.
(48) Attfield, J. P.; Sleight, A. W.; Cheetham, A. K. *Nature* **1986**, *322*, 620−622.

Table 1. Samples Used in XANES Data Analyses[a]

no.	description[b]	ref	no.	description[g]
A1	$[Cr(OH_2)_6](NO_3)_3 \cdot 3H_2O$	41	**B1a,b**	A549 + Cr(VI), 4 h, whole cells[h]
A2	$Na_9[Cr(OH)_6]_2(OH)_3 \cdot 6H_2O$	42	**B2**	A549 + Cr(VI), 2 h, whole cells[i]
A3	*rac*-$[Cr(en)_3]Cl_3 \cdot 3H_2O$	43	**B3**	A549 + Cr(VI), 1 h, whole cells[i]
A4	$K_3[Cr(ox)_3] \cdot 3H_2O$	44	**B4**	A549 + Cr(VI), 20 min, whole cells[i]
A5	$K_3[Cr(cat)_3]$[c]	45,46	**B5**	A549 + Cr(VI), 4 h, whole cells (10 K)[j]
A6	$[Cr(dedtc)_3]$	47	**B6**	A549-DHA + Cr(VI), 4 h, whole cells
A7	$CrPO_4$ (polymeric)	48,49	**B7**	HepG2 + Cr(VI), 4 h, whole cells
A8	*cis*-$[Cr(phen)_2(OH_2)_2](NO_3)_3 \cdot 5/2H_2O$	50	**B8**	V79 + Cr(VI), 4 h, whole cells
A9	*cis*-$[Cr(phen)_2(dpp)_2](NO_3)$	51	**B9**	C2C12 + Cr(VI), 4 h, whole cells
A10	$[Cr(ala)_3] \cdot H_2O$[d]	52,53	**B10**	A549 + Cr(VI), 4 h, nuclei (crude)
A11	$Na[Cr(cys)_2] \cdot H_2O$	54	**B11**	A549 + Cr(VI), 4 h, HMM
A12	$Na[Cr(asp)_2] \cdot 2H_2O$[e]	55	**B12a,b**	A549 + Cr(VI), 4 h, LMM [h]
A13	$[Cr(his)_2](BF_4)$[e]	56	**B13**	A549 + Cr(VI), 4 h, nuclei (purified)
A14	$[Cr(pic)_3] \cdot H_2O$	57	**B14**	A549 lysate + Cr(VI), HMM
A15	*trans*-$Ba[Cr(glyglygly)(OH)_2]$	58	**B15**	A549 HMM + $[Cr(OH_2)_6]^{3+}$
A16	$[Cr_3O(OCOEt)_6(OH_2)_3](NO_3) \cdot 3H_2O$	59	**B16**	A549 HMM + Cr(VI) + GSH
A17	$[Cr_8(OH)_8(OAc)_{16}] \cdot 20H_2O$	40	**B17**	A549 HMM + Cr(VI) + Asc
C	chromodulin[f]	11		

[a] Unless stated otherwise, XANES spectra were acquired at SSRL for solid samples (295 K). Details of sample preparation and data acquisition are given in the Experimental Section. [b] Designations of the ligands in model Cr(III) complexes (**A1**−**A17**): en = 1,2-ethanediamine; ox = oxalato(2−); cat = catecholato(2−); dedtc = diethyldithiocarbamato(1−); phen = 1,10-phenanthroline; dpp = diphenylphosphato(1−); ala = L-alaninato(1−); cys = L-cysteinato(2−); asp = L-aspartato(2−); his = L-histidinato(1−); pic = 2-pyridinecarboxylato(1−); and glyglygly = glycylglycylglycinato(3−). [c] Data were acquired at 10 K for a frozen aqueous solution of the complex (10 mM) in the presence of NaOH (0.10 M),[46] due to the air-sensitivity of the complex under ambient conditions. [d] Data were acquired for a purple water-soluble fraction, probably consisting of a mixture of geometric isomers of $[Cr(ala)_3]$ (Figure S1). [e] Data for mixtures of geometric isomers were used in the analyses; no significant differences in XANES spectra of separate geometric isomers were detected (Figure S2). [f] The published XANES spectrum[11] was used in the data analyses. [g] Designations used for the biological samples (**B1**−**B17**): A549, HepG2, V79, and C2C12 are the cell lines used (see the Experimental Section); A549-DHA are A549 cells, pretreated with dehydroascorbic acid (2.0 mM for 90 min);[64] HMM and LMM are high- and low-molecular-mass fractions (the cutoff for fraction separation was 30 kDa); GSH is glutathione (reduced form) and Asc is ascorbate. [h] Spectra were acquired for two independent preparations of each sample either at SSRL (**B1a**, **B12a**) or at ANBF (**B1b**, **B12b**). [i] Data from previous work[18] were collected at ANBF. [j] A suspension of cells in PBS, frozen in liquid N_2 immediately after the Cr(VI) treatment; data were acquired at 10 K.

elemental analyses (C, H, N, Cr), electrospray mass spectrometry (ESMS), or X-ray powder diffraction measurements (for the insoluble polymeric compound **A7** only). Details of syntheses and characterizations of the model complexes are given in the Supporting Information. Separation of geometric isomers of Cr(III) amino acid complexes was carried out by ion-exchange chromatography according to the published procedures,[55,56] and the identities of isomers were verified by circular dichroism (CD) spectroscopy (Figure S1 in Supporting Information). No significant differences were detected in the XANES spectra of various geometric isomers (Figure S2 in Supporting Information).

Cell Culture and Sample Preparation. The following cell lines were originally received from the American Tissue Culture Collection and cultured for 10−20 passages prior to the experiments: A549 (human lung adenocarcinoma);[60] HepG2 (human hepatoma);[61] V79 (Chinese hamster lung fibroblasts)[62] and C2C12 (mouse myoblasts).[63] The A549, HepG2, and V79 cell lines were cultured in monolayers in Advanced Dulbecco's modified minimal essential medium (DMEM),[64] supplemented with L-glutamine (2.0 mM), antibiotic−antimycotic mixture (100 U mL^{-1} penicillin, 100 mg mL^{-1} streptomycin, and 0.25 mg mL^{-1} amphotericin B), and fetal calf serum (FCS, heat-inactivated, 2% v/v). The cells were seeded at a density of 5×10^5 cells per 100-mm tissue culture dish (10 mL medium), grown to 80−90% confluency at 310 K in a 5% CO_2-humidified incubator, and subcultured every 3−4 days. Similar procedures were used for culturing C2C12 cells, except that the amount of FCS was increased to 10% v/v, and the cells were subcultured at 50% confluency to prevent differentiation.[63] Typical morphologies of the cell lines used are shown in Figure S3, Supporting Information.

Treatments of cell monolayers with Cr(VI) (0.10 mM as Na_2CrO_4 in complete medium for 20 min to 4 h at 310 K) and preparations of bulk cell pellets (~2×10^7 cells per sample; **B1**−**B4** and **B6**−**B9** in Table 1) for X-ray absorption spectroscopy (XAS) were carried out as described previously.[18] Cell pellets were frozen in liquid N_2 (77 K) within 30 min after the removal of Cr(VI), freeze-dried at 217 K and 0.5 mbar for 24 h, and stored desiccated at 277 K for 1−2 weeks prior to analyses. For preparation of a sample of snap-frozen Cr(VI)-treated A549 cells (**B5** in Table 1), cell monolayers were washed with phosphate-buffered saline (PBS, 3 × 20 mL) after the removal of Cr(VI) and collected by scraping into PBS (~2 mL per 150-mm dish). The cells were then allowed to settle by gravity, the resultant thick suspension was mixed with glycerol (30% v/v), and the mixture was loaded into a 200-μL Lucite XAS cell, frozen in liquid N_2 (within 5 min after the removal of Cr(VI)) and stored at 77 K. In one experiment (**B6** in Table 1), a pretreatment of A549 cells with dehydroascorbic acid (2.0 mM in complete medium for 90 min at 310 K) was used to achieve loading of the cells with ascorbate (since human cells in culture do not contain significant amounts of ascorbate).[65] This pretreatment was followed by removal of the dehydroascorbate-containing medium,

(49) Glaum, R.; Gruehn, R.; Möller, M. *Z. Anorg. Allg. Chem.* **1986**, *543*, 111−116.
(50) Weeks, C. L.; Levina, A.; Dillon, C. T.; Turner, P.; Fenton, R. R.; Lay, P. A. *Inorg. Chem.* **2004**, *43*, 7844−7856.
(51) Ferreira, A. D. Q.; Bino, A.; Gibson, D. *Inorg. Chem.* **1998**, *37*, 6560−6561.
(52) Minor, S. S.; Witte, G.; Everett, G. W. *Inorg. Chem.* **1976**, *15*, 2052−2055.
(53) Pedrosa de Jesus, J.; Dos, Santos, T. M.; O'Brien, P. *Polyhedron* **1991**, *10*, 575−577.
(54) De Meester, P.; Hodgson, D. J.; Freeman, H. C.; Moore, C. J. *Inorg. Chem.* **1977**, *16*, 1494−1498.
(55) Watabe, M.; Yano, H.; Odaka, Y.; Kobayashi, H. *Inorg. Chem.* **1981**, *20*, 3623−3627.
(56) Hoggard, P. E. *Inorg. Chem.* **1981**, *20*, 415−420.
(57) Stearns, D. M.; Armstrong, W. H. *Inorg. Chem.* **1992**, *31*, 5178−5184.
(58) Headlam, H. A. The Role of Cr(III) and Cr(V) Peptide and Amino Acid Complexes in Cr-Induced Carcinogenesis. Ph.D. Thesis, The University of Sydney, Sydney, Australia, 1998.
(59) Antsyshkina, A. S.; Porai-Koshits, M. A.; Arkhangel'skii, I. V.; Diallo, I. N. *Russ. J. Inorg. Chem.* **1987**, *32*, 2928−2932; Engl Translation pp 1700−1703.
(60) A549 human lung carcinoma cell line (ATCC Number: CCL-185).
(61) HepG2 human hepatocellular carcinoma cell line (ATCC Number: HB-8065).
(62) V79 Chinese hamster lung fibroblastic cell line (ATCC Number: CCL-93).
(63) C2C12 mouse myoblastic cell line (ATCC Number: CRL-1772).
(64) Advanced DMEM, Cat. No. 12491-015., Gibco, Invitrogen Corp.
(65) Quievryn, G.; Messer, J.; Zhitkovich, A. *Biochemistry* **2002**, *41*, 3156−3167.

repeated washings with PBS, and addition of fresh Cr(VI)-containing medium. In all cases, Cr(VI) treatments did not cause visible changes in cell morphology. Aliquots of cell culture media (1.0 mL) after the Cr(VI) treatments were also collected and freeze-dried for XANES spectroscopy, which confirmed the absence of any significant reduction of Cr(VI) in the cell culture medium for at least 4 h at 310 K[18,21] (Figure S4, Supporting Information).

For separation of subcellular fractions, Cr(VI)-treated or untreated A549 cells ($\sim 5 \times 10^7$ cells per sample) were lysed for 15 min at 273 K in lysis buffer 1 (LB1, 5.0 mL), containing 4-(2-hydroxyethyl)-1-piperazineethanesulfonic acid (HEPES, 10 mM, pH 7.4), phenylmethylsulfonyl fluoride (PMSF, a protease inhibitor, 1.0 mM), and Triton X-100 (1.0% w/v). Crude nucleic fraction (**B10** in Table 1) was separated by centrifugation (1000*g* for 5 min at 277 K) and then washed with 1.0 mL of LB1. The supernatant was filtered through Microcon YM 30 membrane filters (Millipore; 30 kDa cutoff; volume, 0.50 mL) by centrifugation (14000*g* for 30 min at 277 K). The residue on the filters was washed with LB1 (0.50 mL per filter), dissolved in H_2O (0.10 mL per filter), and freeze-dried to obtain the high-molecular-mass (HMM) cytoplasmic fraction (**B11** in Table 1). Similarly, the nucleic pellet and the filtrate after membrane filtration were freeze-dried to obtain the nucleic and low-molecular-mass (LMM) cytoplasmic fractions, respectively (**B10** and **B12** in Table 1). Prior to the freeze-drying, aliquots (1/50) of each fraction (**B10**−**B12**) were taken for the determination of Cr content by graphite furnace atomic absorption spectroscopy (GFAAS), as described previously.[18] An alternative procedure for separation of cell nuclei (**B13** in Table 1)[66,67] involved the lysis of Cr(VI)-treated A549 cells ($\sim 5 \times 10^7$ cells per sample, 5 min at 0 °C, with vigorous shaking) in lysis buffer 2 (LB2, 10 mL), containing NaCl (10 mM), $MgCl_2$ (5.0 mM), Tris (10 mM, pH 7.0), and Nonidet P-40 (0.5% w/v). The nucleic pellet was separated by centrifugation (1000*g* for 5 min at 277 K) and purified by another treatment with LB2 (10 mL, 5 min at 273 K), followed by recentrifugation. Microscopic examination of the pellets, isolated by either of the lysis techniques, showed clusters of round-shaped nuclei, uniformly stained by trypan blue,[67] with occasional inclusions of cell membrane fragments (Figure S3).

The reaction of the cell lysate (total cytoplasmic fraction), obtained from untreated A549 cells ($\sim 3 \times 10^7$ cells lysed in 3.0 mL of LB1), with Cr(VI) (Na_2CrO_4, 0.10 mM) was carried out for 72 h at 277 K, followed by the separation of Cr(III)-containing HMM fraction as described above (**B14** in Table 1). In order to ensure the complete removal of unbound Cr(VI) and Cr(III), the residue on the filter was washed twice with aqueous Na_2SO_4 (10 mM, 0.50 mL per filter)[68] and then twice with water. The HMM cytoplasmic fraction, isolated from untreated A549 cells (as described above), was used for the in vitro reactions with Cr compounds (0.10 mM of Cr(VI) or Cr(III), **B15**−**B17** in Table 1). For these reactions, the HMM fraction of untreated A549 cells ($\sim 5 \times 10^7$ cells) was dissolved in HEPES-buffered saline (HBS, containing 20 mM HEPES, pH 7.4, 140 mM NaCl, 5.0 mM KCl, 2.5 mM $MgCl_2$, and 1.0 mM $CaCl_2$)[69] to give total protein concentration of 5.0 mg mL^{-1} (determined spectrophotometrically with Coomassie blue stain, using bovine serum albumin as a standard).[70] The reactions were carried out for 15 h at 310 K, after which the Cr(III)-containing HMM fraction was isolated by membrane filtration, washed with H_2O (2×0.5 mL per filter) and freeze-dried.

EPR Spectroscopy. X-band EPR spectra were recorded on a Bruker EMX spectrometer that was equipped with an EMX 035 NMR gaussmeter and an EMX 048T microwave bridge controller. For the studies of Cr(V) intermediate formation during the reactions of Cr(VI) with mammalian cells (A549, HepG2, V79, and C2C12 cell lines), untreated cells ($\sim 2 \times 10^7$ per sample) were collected by trypsinization (0.25% trypsin in PBS for 10 min at 310 K) and resuspended in HBS (0.25 mL), containing Cr(VI) (0.50 mM Na_2CrO_4). The suspension was placed into a flat quartz EPR cell, and several spectra were acquired within 1 h after the beginning of the Cr(VI) treatment (295 K). At least 90% of the cells retained their membrane integrity after the EPR experiments, as shown by trypan blue staining.[71] The instrumental parameters were as follows: microwave frequency, ~9.67 GHz; microwave power, 20 mW; modulation frequency, 100 G; modulation amplitude, 1 G; scan range, 3380−3580 G; resolution, 1024 points; time constant, 20.5 ms; receiver gain, 5×10^5; number of scans, 20. For low-temperature (77 K) EPR spectroscopy of the LMM fraction of Cr(VI)-treated A549 cells, a freeze-dried sample (**B12b** in Table 1, after XAS experiments) obtained from $\sim 5 \times 10^7$ cells was dissolved in 0.40 mL of H_2O (the resultant Cr concentration was 0.75 mM, as determined by GFAAS), and the mixture was transferred into a quartz EPR tube, frozen in liquid N_2, and placed into a "coldfinger" liquid N_2 dewar within the cavity of the EPR spectrometer. The instrumental parameters were as follows: microwave frequency, ~9.27 GHz; microwave power, 20 mW; modulation frequency, 100 G; modulation amplitude, 5 G; scan range, 50−6950 G; resolution, 1024 points; time constant, 81 ms; receiver gain, 5×10^5; number of scans, 20. Processing of EPR data was performed with the use of WinEPR software.[72]

X-ray Absorption Spectroscopy (XAS) and Data Analyses. Chromium K-edge spectra of the cell-derived samples and model Cr(III) complexes were recorded at beamline 9−3 at the Stanford Synchrotron Radiation Laboratory (SSRL) or at the Australian National Beamline Facility (ANBF, beamline 20B at the Photon Factory, Tsukuba, Japan). The beam energy was 3.0 GeV (SSRL) or 2.5 GeV (ANBF), and the maximal beam current was 100 mA (SSRL) or 400 mA (ANBF). Beamline 9-3 at SSRL had a double-crystal Si[220] monochromator, an upstream collimating mirror, and a downstream sagittally focusing mirror; both mirrors were Rh-coated and also provided harmonic rejection. Harmonic rejection was achieved at ANBF by detuning the channel-cut Si[111] monochromator by 50%. Neat freeze-dried samples or mixtures of model complexes with BN (boron nitride) (~1:10 w/w) were pressed into 0.5-mm pellets that were supported within an Al spacer between two 63.5-μm Kapton tape windows (window size, 2×10 mm), and XAS data were recorded at 295 K. Oily samples (**B12a**,**b** in Table 1) were absorbed on pieces of filter paper (10×10 mm) that were attached to Al sample holders with Kapton tape. Low-temperature XAS measurements could not be used satisfactorily for most of the biological samples due to the low Cr concentrations and strong absorption of photons at the ~6 keV energy range by cryostat windows.[18] All the biological samples used in this work, except for **B5**, were freeze-dried, since this technique simplified sample handling, made room-temperature XANES measurements possible, and led to stronger signals. In some cases (**A5** and **B5** in Table 1), XAS of frozen liquid samples were acquired at 10 K (at SSRL), using Lucite sample cells (200 μL) and a continuous-flow liquid He cryostat. All XAS data were acquired in fluorescence detection mode, using a 30-element Ge-array detector (Canberra Industries) at SSRL or a 36-pixel Ge planar detector (Eurisys) at ANBF. For most samples, XANES spectra were recorded at SSRL over the 5770−6130 eV energy range (step sizes, 10 eV below 5970 and 0.25 eV above 5970 eV). The energy scale was calibrated using a stainless steel foil as an internal standard (calibration energy, 5989.0 eV, corresponded

(66) Farrell, R. E., Jr. *RNA Methodologies: a Laboratory Guide for Isolation and Characterization*; Academic Press: San Diego, CA, 1998; pp 406−437.
(67) Nuclei Isolation Kit (technical bulletin), Product No. NUC-101, Sigma.
(68) Levina, A.; Harris, H. H.; Lay, P. A. *J. Biol. Inorg. Chem.* **2006**, *11*, 225−234.
(69) Sarabia, V.; Ramlal, T.; Klip, A. *Biochem. Cell. Biol.* **1990**, *68*, 536−542.
(70) Bio-Rad Protein Assay (technical bulletin), Cat. No. 500-0002., Bio-Rad Laboratories.
(71) Freshney, R. I. *Culture of Animal Cells, a Manual of Basic Technique*, 4th ed.; Wiley-Liss: New York, 2000; pp 330−331.
(72) *WinEPR*, Version 960801 (1996) Bruker-Franzen Analytic, Bremen, Germany.

to the first peak of the first derivative of Cr(0) edge).[73] Two sequential scans were recorded for each sample (scan time, 15 min), and the absence of noticeable photodamage of the samples was confirmed from the lack of significant spectral changes between the scans (e.g., the difference in edge energies did not exceed 0.1 eV).[74,75] For some of the samples with relatively high Cr content (**B1b** and **B12b** in Table 1), XANES and XAFS spectra were recorded at ANBF, using the following energy ranges: preedge region, 5770−5970 eV (10 eV steps); XANES region, 5970−6050 eV (0.25 eV steps), and XAFS region, 6050−7000 eV (0.05 $Å^{-1}$ steps in *k*-space). For these samples, four to five sequential scans were recorded (scan time, 40 min), and the lack of appreciable photodamage was established from the absence of significant changes in XANES spectra of sequential scans.[74,75] The possibility of sample photodamage is generally lower at ANBF compared with SSRL due to a lower photon flux.[75]

Calibration, averaging, and splining of XANES data, as well as target transformation analyses,[32] were performed using the EXAFSPAK software package.[76] Principal component and multiple linear regression analyses of XANES data[25,26,31] for Cr(III) in biological samples (**B1**−**B17** and **C** in Table 1) were performed using Unscrambler[77] and Origin[78] software, respectively. Multiple-scattering fittings of XAFS data[30,74,75] were performed using the XFIT software package,[79] based on the FEFF8 code.[80] Overdetermined models ($N_i/p > 1$, where N_i is the number of independent observations and p is the number of varied parameters) were used in XAFS calculations, which allowed meaningful solutions to be obtained.[81] Published XANES, XAFS, and EPR data[11] were digitized using the WinDig software[82] for comparison with the data obtained in this work.

Results

Comparison of XANES Spectra for Biological and Model Samples. From the previous work,[18,21,22,36−39] Cr(III) was expected to be the predominant oxidation state in Cr(VI)-treated mammalian cells and subcellular fractions (**B1**−**B17** in Table 1). Accordingly, the models used (**A1**−**A17** in Table 1) included Cr(III) complexes with a wide range of donor groups that can potentially be found in biological systems: H_2O (**A1**, **A8**, and **A16**); OH^- (**A2** and **A15**); RR′R″N (amine, **A3**, **A10**−**A13**, **A15**); $RCOO^-$ (**A4**, **A10**−**A15**); RO^- (catecholato, **A5**); RS^- (**A6** and **A11**), RR′S (**A6**); μ-PO_4^{3-} (**A7**); RR′N (imine, **A8**, **A9**, **A13**, and **A14**); $(RO)_2PO_2^-$ (**A9**); $RR'N^-$ (amido, **A15**); μ^3-O^{2-} (**A16**); μ-OH^- (**A17**); and μ-$RCOO^-$ (**A16** and **A17**). All the model complexes used possess six-coordinate octahedral geometry, as do nearly all known Cr(III) complexes.[83] An overview of XANES spectra of the model complexes (Figure S5 in Supporting Information) shows a strong dependence of the edge shapes and postedge absorbance features on the nature

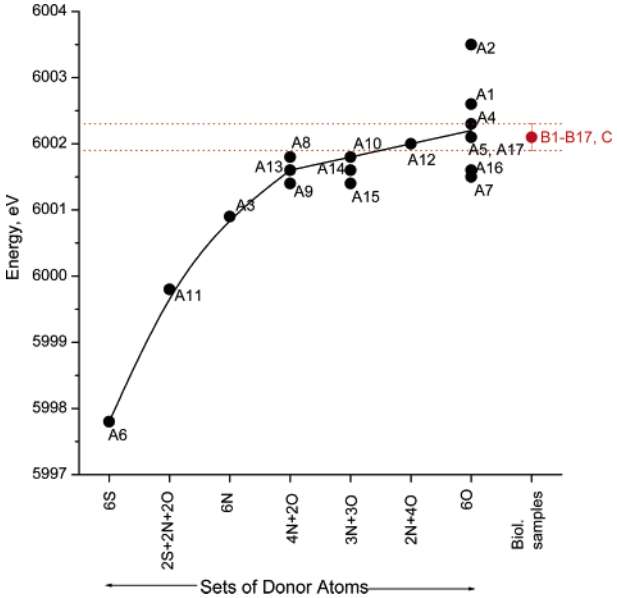

Figure 1. Comparison of edge energies (measured at half-height of the edge jump) in XANES spectra of biological samples and model Cr(III) complexes. Designations of the samples correspond to Table 1.

of donor groups in Cr(III) complexes. As expected,[84] increasing the electronegativity of donor atoms (S < N < O) led to increases in edge energies (measured at half-height of the edge jump) for the model Cr(III) complexes, although the changes for the complexes with various *O*/*N*-donor atom sets were not as pronounced as those for the *S*-donor-containing complexes (Figure 1). By contrast with the range of energies and shapes in the model complexes, XANES spectral shapes for most of the cell-derived samples (**B1**−**B17** in Table 1) were similar, as were the edge energies (6002.1 ± 0.2 eV, Figure 1).

Most of the biological samples (**B1**−**B7** and **B10**−**B17** in Table 1) were derived from a human lung epithelial cell line (A549),[60] which is a commonly used model in studies of Cr(VI)-induced carcinogenesis (since the lung is the main site of cancers caused by occupational exposure to Cr(VI)).[2,9,10] A human hepatic cell line (HepG2),[61] since chromodulin was prepared from the reaction of Cr(VI) with liver homogenate, and two rodent cell lines (V79 and C2C12)[62,63] were used for comparison (samples **B7**−**B9** in Table 1). The samples included the following: (i) whole Cr(VI)-treated cells (either freeze-dried or snap-frozen; **B1**−**B9** in Table 1); (ii) subcellular fractions of Cr(VI)-treated cells (**B10**−**B13** in Table 1); (iii) subcellular fractions of untreated cells, reacted with Cr(VI) or Cr(III) compounds (**B14**−**B17** in Table 1).

Representative examples of XANES spectra of biological samples (samples **B1a**, **B12a**, **B12b**, and **C**) are given in Figure 2, and the rest of the spectra are shown in Figure S6, Supporting Information. A comparison of the edge energy values for the model and biological Cr(III) samples (Figure 1) suggests the predominance of Cr−O coordination and the absence of any significant Cr−S coordination in the latter samples. The preedge absorbance intensities in XANES spectra of samples **B1**−**B17** did not exceed those for the model Cr(III) complexes (**A1**−**A17**, Figure S5), which points to the absence of detectable amounts of Cr(VI) or Cr(V) oxo complexes in the cell-derived

(73) Thompson, A. C.; Attwood, D. T.; Gullikson, E. M.; Howells, M. R.; Kortright, J. B.; Robinson, A. L.; Underwood, J. H.; Kim, K-J.; Kirz, J.; Lindau, I.; Pianetta, P.; Winick, H.; Williams, G. P.; Scofield, J. H. *X-Ray Data Booklet*, 2nd ed.; University of California: Berkeley, CA, 2001.
(74) Rich, A. M.; Armstrong, R. S.; Ellis, P. J.; Freeman, H. C.; Lay, P. A. *Inorg. Chem.* **1998**, *37*, 5743−5753.
(75) Levina, A.; Codd, R.; Foran, G. J.; Hambley, T. W.; Maschmeyer, T.; Masters, A. F.; Lay, P. A. *Inorg. Chem.* **2004**, *43*, 1046−1055.
(76) George, G. N. *EXAFSPAK*, Stanford Synchrotron Research Laboratory, Stanford, CA, 2001.
(77) *Unscrambler*, Version 9.5 (2005) Camo Process AS, Oslo, Norway.
(78) *Microcal Origin* Version 6.0 (1999), Microcal Software Inc., Northampton, MA.
(79) *XFit* for Windows, beta-version. Australian Synchrotron Research Program, Sydney, Australia, 2004.
(80) Ankudinov, A. L.; Ravel, B.; Rehr, J. J.; Conradson, S. D. *Phys. Rev. B* **1998**, *58*, 7565−7576.
(81) Binsted, N.; Strange, R. W.; Hasnain, S. S. *Biochemistry* **1992**, *31*, 12117−12125.
(82) Lovy, D. *WinDIG*, University of Geneva, Geneva, Switzerland, 1996.
(83) Lay, P. A.; Levina, A. In *Comprehensive Coordination Chemistry II*; McCleverty, J. A.; Meyer, T. J. Eds.; Elsevier: Oxford, UK 2004; Vol. 4, pp 313−413.
(84) Solomon, E. I.; Hedman, B.; Hodgson, K. O.; Dey, A.; Szilagyi, R. K. *Coord. Chem. Rev.* **2005**, *249*, 97−129.

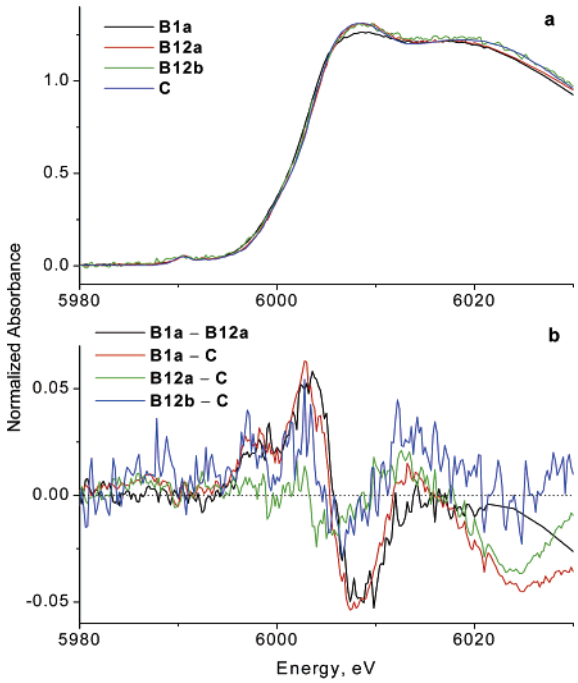

Figure 2. Comparison of XANES spectra (a) and difference XANES spectra (b) of Cr(III) in cell-derived samples (**B1a**, **B12a**, and **B12b**, Table 1) and published data for chromodulin (**C**).[11] Alternative splining and normalization algorithms were used for **B12a** (EXAFSPAK software)[76] and **B12b** (XFIT software).[79] The chromodulin figure was reproduced with permission from ref 11.

samples.[18,22] These results were not due to the photoreduction of Cr(VI/V) oxo complexes during the XAS data acquisition,[75] as confirmed by the observation of unaltered XANES spectra of Cr(VI) in the freeze-dried cell culture medium samples at 295 K (Figure S4). By contrast, the formation of Cr(V) and Cr(VI) species in Cr(III)-treated adipocytes has been recently detected by microprobe XANES spectroscopy.[16] No high oxidation states of Cr were detected even when the treated cells were stored at 77 K from ~5 min after the removal of Cr(VI) until the XAS experiment at 10 K (sample **B5** in Table 1). Although the Cr content in **B5** was among the highest from all the biological samples (**B1**−**B17** in Table 1),[18] the signal-to-noise ratio in the corresponding XANES spectrum was low compared to those of typical freeze-dried samples (Figure S6), due to the high H_2O content in **B5** and attenuation of the signal by the cryostat windows (see the Experimental Section).

A detailed comparison of XANES spectra for samples **B1**−**B17**, including overlays and difference spectra, is shown in Figures 2 and S6. For the following samples (Table 1), the observed spectral differences did not exceed double the experimental noise levels: (i) identical but independent preparations of Cr(VI)-treated A549 cells (**B1a**,**b**) or LMM cellular fractions (**B12a**,**b**), when the data were acquired at different synchrotron sources (SSRL or ANBF); (ii) samples of Cr(VI)-treated (0.10 mM for 4 h at 310 K) A549 cells, prepared either by freeze-drying (**B1a**, data acquired at 295 K) or by snap-freezing (**B5**, data acquired at 10 K); (iii) A549 cells, treated with Cr(VI) (0.10 mM) for various times at 310 K (4, 2, or 1 h or 20 min, **B1b** and **B2**−**B4**, data acquired at ANBF);[18] (iv) various cell lines (A549, HepG2, V79, or C2C12) treated with Cr(VI) (0.10 mM for 4 h at 310 K), as well as A549 cells, loaded with ascorbate prior to the Cr(VI) treatment (**B1a** and **B6**−**B9**); and (v) whole Cr(VI)-treated A549 cells and nucleic or HMM (>30 kDa) fractions isolated from such cells (**B1a**, **B10**, **B11**, and **B13**). The absence of significant differences in XANES spectra of **B1a** (a freeze-dried sample) and **B5** (a snap-frozen cell suspension; see the Experimental Section) justifies the use of freeze-dried samples for the studies of Cr(III) speciation in Cr(VI)-treated cells and subcellular fractions (Table 1). The following preparations, derived from A549 cells (Table 1), showed significant differences in XANES spectra compared with the samples of whole Cr(VI)-treated cells (**B1a**,**b**; see Figures 2 and S6): (i) the LMM (<30 kDa) fraction isolated from Cr(VI)-treated cells (**B12a**,**b**); (ii) the HMM fraction isolated from the reaction of the cell lysate with Cr(VI) (**B14**); and (iii) the HMM fraction of untreated cells after in vitro reactions with Cr(III) (**B15**) or with Cr(VI) in the presence of biological reductants (glutathione or ascorbate, **B16** and **B17**). These observations were confirmed by the results of principal component analysis,[31,32,77] showing clustering of the samples **B1**−**B11** and **B13** and significant differences for the samples **B12a**,**b** and **B14**−**B17** (Figure S7 in Supporting Information).

Modeling of XANES Spectra of Cr(III) in Biological Samples. Likely average coordination environments of Cr(III) in cell-derived samples (**B1**−**B17** in Table 1) were determined using multiple linear regression fitting of their XANES spectra with those of model Cr(III) complexes (**A1**−**A17** in Table 1).[25,26,39] The following criteria were used to define a successful fit: (i) the regression coefficients for all the components in the model were positive; (ii) the calculated probability values for the presence of each of the components exceeded 99.9% (P <0.001);[78] (iii) the exclusion of any component from the model led to a noticeable increase in the fit residue (exceeding that of the experimental noise level). The two best fits for each of the samples (models 1 and 2) are listed in Table 2, and calculated spectra and fit residues for the alternative models are shown in Figure 3a (sample **B1b**) and in Figure S8, Supporting Information.

Most of the model Cr(III) complexes (**A1**−**A17** in Table 1) and, hence, donor groups were excluded from the analyses due to negative regression coefficients, with only six model complexes being required to fit the range of XANES (Table 2). Of these, Cr(III) complexes with non-sulfur-containing amino acid ligands (alanine, aspartate and histidine; **A10**, **A12**, and **A13** in Table 1) were the dominant components of nearly all of the models (Table 2). These results were consistent with target transformation analyses[31,32,76] (Table S1, Supporting Information), showing that **A10**, **A12**, and **A13** were the most likely components of the target spectra (**B1**−**B17**). The best fits for most of the cell samples (Model 1 for **B1** and **B2** and **B6**−**B11** in Table 2) were similar and included **A12** and **A13** as the major components and **A2** as the minor component. Despite the relatively low molar ratio of the **A2** component (~10−15%, Table 2), it showed high significance (t) values in the regression analyses,[78] and its removal led to significant deteriorations of the fits (an example for **B1a** is shown in Figure S8). Deviations from the "base" model (**A2** + **A12** + **A13**) were observed for samples **B3**, **B4**, **B5**, and **B13** (Tables 1 and 2), but these results were inconclusive, since the improvements in the fits were comparable with the experimental noise (Figure S8). Notably, **B3** (A549 cells treated with 0.10 mM Cr(VI) for 1 h at 310 K, Table 1) was the only whole-cell sample to show a slight

Table 2. Results of Multiple Linear Regression Modeling of XANES Spectra of Cr(III) in Cr(VI)-Treated Cells and Subcellular Fractions[a]

	model 1						model 2		
sample	**A1**	**A2**	**A12**	**A13**	**A17**	R^2	**A10**	**A12**	R^2
B1a		0.12(1)	0.44(2)			0.99983	0.46(2)	0.54(2)	0.99975
B1b		0.14(1)	0.38(1)	0.48(1)		0.99993	0.48(2)	0.52(2)	0.99978
B2		0.14(1)	0.39(3)	0.47(3)		0.99953	0.41(3)	0.59(3)	0.99927
B3		0.10(1)	0.31(2)	0.35(2)	0.24(2)	0.99985	0.60(2)	0.40(2)	0.99967
B4		0.15(1)		0.85(1)		0.99882	1.00(2)		0.99901
B5	0.32(2)		0.34(3)	0.34(3)		0.99933	0.62(5)	0.38(5)	0.99873
B6		0.13(1)	0.37(2)	0.50(2)		0.99979	0.52(2)	0.48(2)	0.99972
B7		0.16(1)	0.40(1)	0.44(1)		0.99991	0.38(3)	0.62(3)	0.99957
B8		0.16(1)	0.27(2)	0.57(2)		0.99986	0.56(2)	0.44(2)	0.99966
B9		0.15(1)	0.40(2)	0.45(2)		0.99986	0.44(2)	0.56(2)	0.99963
B10		0.18(1)	0.22(2)	0.60(2)		0.99961	0.57(4)	0.43(4)	0.99928
B11		0.14(1)	0.41(2)	0.45(2)		0.99968	0.47(3)	0.53(3)	0.99953
B12a	0.39(1)	0.16(1)	0.45(2)			0.99957	0.48(6)	0.52(6)	0.99784[b]
B12b	0.40(1)	0.08(1)	0.52(2)			0.99946	0.50(6)	0.50(6)	0.99835[b]
B13	0.08(1)	0.15(1)		0.61(1)	0.16(2)	0.99986	0.77(3)	0.23(3)	0.99959
B14		0.14(1)		0.20(3)	0.66(3)	0.99952	0.80(6)	0.20(6)	0.99836[b]
B15		0.30(1)		0.70(2)		0.99889[b]	0.86(8)	0.14(8)	0.99680[b]
B16		0.24(1)		0.76(1)		0.99861	1.00(1)		0.99769[b]
B17		0.26(3)		0.74(3)		0.99211[b]	1.00(1)		0.98926[b]
C	0.38(2)	0.11(1)	0.51(2)			0.99934	0.18(6)	0.82(6)	0.99770[b]

[a] Shown in the table are calculated molar components of each of the contributing model complexes (errors in the last significant figures are given in the parentheses) and the correlation coefficients (R^2). Designations of the samples and model complexes correspond to those in Table 1. Experimental and calculated spectra and fit residues are shown in Figure S8. [b] The shapes of the calculated spectra are significantly different from those of the experimental spectra (Figure S8).

improvement in the fit when **A17** (a polynuclear hydroxo-carboxylate, Table 1) was included into the model (Table 2 and Figure S8). This observation is consistent with the detection of Cr...Cr interactions in the XAFS spectrum of the sample **B3** (reported previously).[18] The average Cr−Cr distances in **B3**, calculated by single-scattering fitting of the XAFS spectrum, were close to those in **A17**.[18]

In addition to the three-component model (**A2** + **A12** + **A13**, model 1 in Table 2), good fits for most of the samples (**B1**−**B11** and **B13**) were obtained with the use of only two model components, **A10** and **A12** (model 2 in Table 2). However, inclusion of the **A2** component into the models led to a consistent improvement in the fits for all of the samples, except for **B4** (compare the R^2 values for the models 1 and 2 in Table 2 and the fit residues in Figure S8). Notably, inclusion of **A2** into the regression analyses led to the exclusion of **A10** in favor of **A13**.

In agreement with visual comparisons and principal component analyses of XANES spectra, the largest differences in models compared with the whole-cell samples (such as **B1a**) were observed for the LMM fractions isolated from Cr(VI)-treated cells (**B12a**,**b**) and for the products of the in vitro reactions of Cr compounds with cell lysates (**B14**-**B17**). Regression results (Table 2) point to significant increases in the proportion of hydrolysis-related donor groups (aqua, hydroxo, or bridging carboxylato; models **A1**, **A2**, or **A17**, respectively) in such samples compared with those of whole Cr(VI)-treated cells.

In addition to the models using well-characterized Cr(III) complexes (Table 2), a XANES spectrum of whole Cr(VI)-treated A549 cells (**B1a**) was fitted with a combination of the spectra of subcellular fractions isolated from such cells. The distribution of Cr between the subcellular fractions, as measured by GFAAS, was as follows: nucleic fraction (**B10**), 13 ± 2%; HMM fraction (**B11**), 29 ± 4%; and LMM fraction (**B12a**), 57 ± 5% ($n = 3$). A "reconstructed" spectrum of Cr(III) in whole Cr(VI)-treated cells, based on this distribution (**B1*** = 0.13**B10** + 0.29**B11** + 0.57**B12a**), was significantly different from that observed experimentally (Figure S6f in Supporting Information). The main difference between the spectra of **B1a** and **B1*** (as well as between those of **B1a** and **B12a,b**, Figure 2) was in the edge position, which is sensitive to the nature of the donor groups (Figure 1)[84] and points to changes in the coordination environment of Cr(III) during the cell lysis.

Multiple-Scattering Modeling of XAFS Spectra of Cr(VI)-Treated Cells. Previous XAFS spectroscopic studies of Cr(VI)-treated A549 cells[18] revealed time-dependent changes in the spectra, which were attributed to a decrease in Cr−Cr interactions at longer treatment times. In the present study, more detailed XAFS data analysis was performed for a sample of A549 cells treated with Cr(VI) (0.10 mM) for 4 h at 310 K (**B1b** in Table 1), i.e., under the conditions when no significant effect of Cr−Cr interactions on the spectra was expected.[18] In the previous study,[18] only single-scattering (SS) XAFS modeling was possible, due to the lack of knowledge on the nature of Cr(III)-binding ligands. In this work, multiple-scattering (MS) XAFS models of the most likely Cr(III) binding sites in Cr(VI)-treated cells were proposed, based on the results of XANES data modeling, namely H-free forms of triacetatobis(ethylamine)imidazole-chromium(III) and tetraacetatobis(ethylamine)-chromium(III) (models 1 and 2 in Table 2 and Chart 1). These models lead to equally good fits (R = 13.6% and 14.0% for models 1 and 2, respectively)[79] of the XAFS spectrum for the sample **B1b**. The fitting results for model 1 (Chart 1) are shown in Figure 3b,c, those for model 2 are shown in Figure S9 (Supporting Information), and details of the applied multiple-scattering (MS) XAFS models are given in Tables S2−S4, Supporting Information. The values of bond lengths and angles in the ligands were restrained during the calculations to be within 0.02 Å and 2°, respectively,[30,74] to those determined by X-ray crystallography for Cr(III) amino acid complexes (Table S2).[54,85]

The optimized values of the Cr−ligand bond lengths (1.95−1.96 Å for Cr−O and 2.02−2.04 Å for Cr−N, Table S3) are in

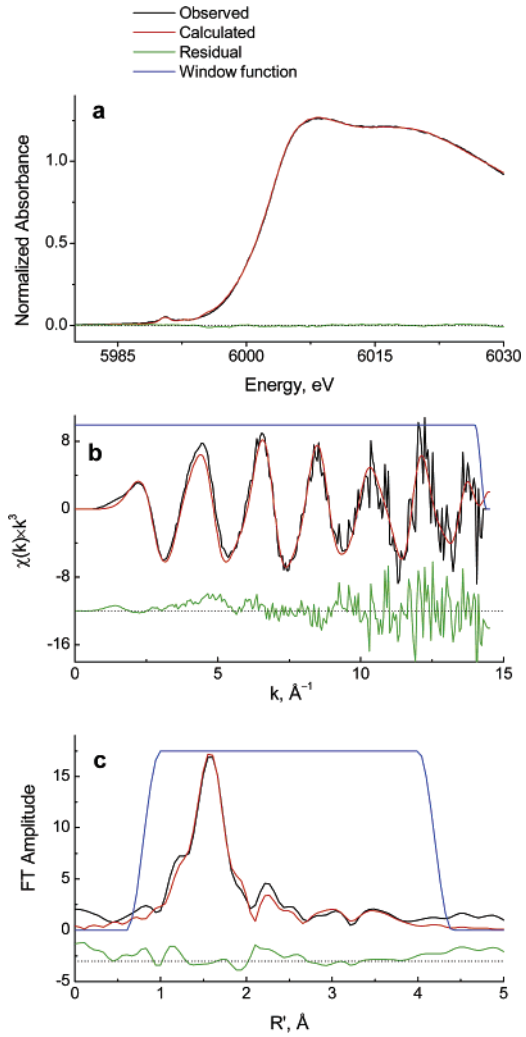

Figure 3. Experimental and calculated XANES (a), XAFS (b), and Fourier transform (FT) XAFS (c) spectra of Cr(VI)-treated A549 cells (sample **B1b** in Table 1). Calculations were performed according to model 1 in Table 2 (for the XANES spectra) or in Chart 1 (for the XAFS spectra). Details of the XAFS calculations are given in the Tables S2−S4, Supporting Information.

agreement with the X-ray crystallography data[54,85] (these values, as well as those of bond angles around the Cr(III) ion, were not restrained during the calculations). No significant differences in the MS XAFS fits were observed for various geometric isomers of the proposed models (similarly to other Cr(III) complexes with carboxylato ligands).[75] Thus, MS XAFS data fitting for the sample **B1b** (Figure 3b,c and S9 and Tables S2−S4) supported the results of XANES data modeling (Table 2), pointing to preferential binding of Cr(III) to amino acid residues in Cr(VI)-treated mammalian cells, but it did not distinguish between two of the possible coordination modes (models 1 or 2 in Chart 1).

Comparison of Spectral Data for Cr(VI)-Treated A549 Cells and Chromodulin. As shown in Figure 2, XANES spectra of two independent preparations of the LMM (<30 kDa) fraction of Cr(VI)-treated A549 cells (**B12a,b** in Table 1), acquired at different synchrotron sources (SSRL or ANBF) and processed with the use of different software,[76,79] were not significantly

Chart 1. Models Used in MS XAFS Fitting of the Coordination Environments of Cr(III) in Cr(VI)-Treated A549 Cells (sample **B1b** in Tables 1 and 2)

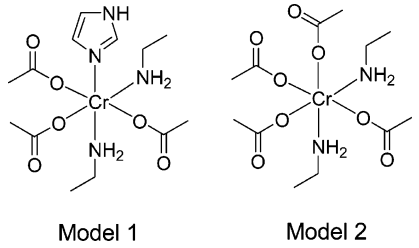

Model 1 Model 2

different (in the 5980−6020 eV range) from that of the published XANES spectrum of chromodulin[11] (**C** in Table 1 and Figure 2). A slight difference between samples **B12a** and **C** at >6020 eV (Figure 1b) was probably due to a difference in the background subtraction procedures.[86] A close similarity of the XANES spectra of **B12a**,**b** and **C** was confirmed by principal component analyses (showing a close correlation between the samples **B12a**, **B12b**, and **C**, Figure S7) and by similar models for these samples obtained from the regression analyses (Table 2).

The X-band EPR spectrum of **B12b** (77 K, frozen aqueous solution) possessed a dominant broad signal at $g \sim 2$ and two weak signals at $g \sim 5$, similarly to the reported EPR spectrum of **C** at 4 K[11] (Figure 4a). The XAFS and Fourier transform (FT) XAFS spectra of **B12b** (a freeze-dried solid at 295 K) also closely matched the corresponding spectra of **C** (frozen aqueous solution; 15 K),[11] as shown in Figure 4b,c. The published results of SS XAFS data analyses for chromodulin[11] suggested the presence of six O/N donor atoms in the first coordination shell of Cr(III) (at an average distance of 1.98(2) Å), five C atoms in the second coordination shell (average Cr...C distance, 3.12-(2) Å), and two different Cr−Cr shells (0.5Cr−Cr at 2.79(2) Å and 1Cr−Cr at 3.79(2) Å). However, SS XAFS fittings are likely to overestimate the degree of Cr−Cr interactions in biological Cr(III) complexes, since they do not take into account the MS contributions from carboxylato groups, which are probably the most abundant donor groups for Cr(III) in biological media, as shown by the XANES and XAFS data fittings for the sample **B1b** (Table 2, Chart 1 and Figure 3b,c). No attempts of MS XAFS data analyses for **B12b** were made, since this sample probably represents a mixture of hydrolysis products of Cr(III)−protein complexes (see Discussion). In summary, XANES, XAFS, and EPR spectroscopic data (Figures 2 and 4) point to a close similarity of the coordination environment of Cr(III) in chromodulin to that in the LMM fraction isolated from Cr(VI)-treated A549 cells (samples **B12a**,**b**) but not to that in the intact cell samples (**B1a**,**b**).

EPR Spectroscopy of Cells during the Cr(VI) Uptake. In agreement with previous studies,[87,88] X-band EPR signals of Cr(V) intermediates in Cr(VI)-treated cells at 295 K could only be observed during the reactions of concentrated cell suspensions ($\sim 2 \times 10^7$ cells in 0.25 mL HBS) with high concentrations of Cr(VI) (≥0.50 mM). Typical spectra for various cell lines are

(85) Madafiglio, K.; Manning, T. M.; Murdoch, C. M.; Tulip, W. R.; Cooper, M. K.; Hambley, T. W.; Freeman, H. C. *Acta. Crystallogr.* **1990**, *C46*, 554−561.
(86) Weng, T.-C.; Waldo, G. S.; Penner-Hahn, J. E. *J. Synchrotron Rad.* **2005**, *12*, 506−510.
(87) Sugiyama, M.; Tsuzuki, K.; Hidaka, T.; Ogura, R.; Yamamoto, M. *Biol. Trace Elem. Res.* **1991**, *30*, 1−8.
(88) Witmer, C.; Faria, E.; Park, H. -S.; Sadrieh, N.; Yurkow, E.; O'Connell, S.; Sirak, A.; Schleyer, H. *Environ. Health. Perspect. Suppl. 3* **1994**, *102*, 169−176.

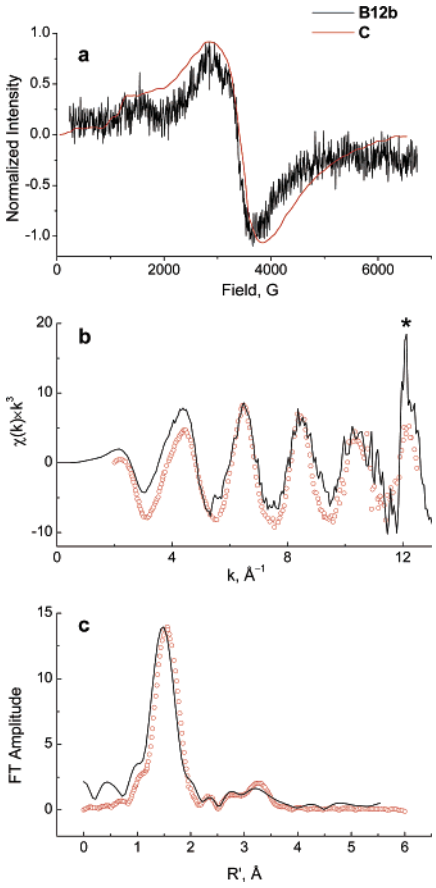

Figure 4. Comparison of EPR (**a**), XAFS (**b**) and FT XAFS (**c**) spectra of the LMM fraction of Cr(VI)-treated A549 cells with the literature data for chromodulin[11] (samples **B12b** and **C** in Table 1). A feature designated with an asterisk is an artifact due to the trace Mn absorption edge.[73] The FT XAFS spectrum for the sample **B1b** (black line in **c**) was obtained by limiting the *k* range to 12 Å^{-1}. The chromodulin figures were reproduced with permission from ref 11.

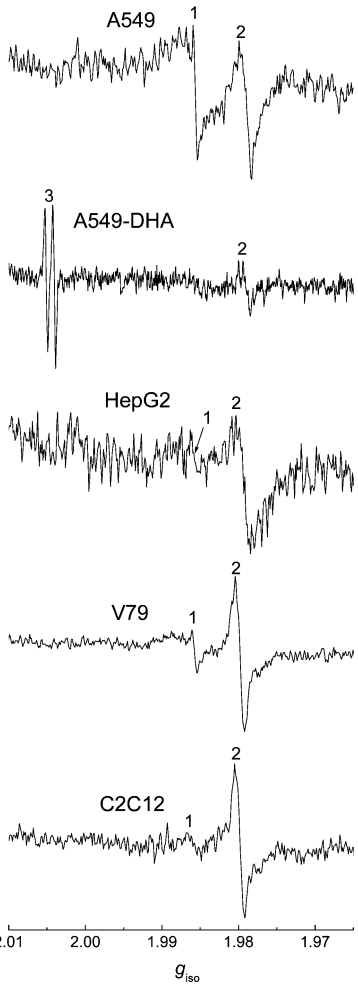

Figure 5. X-band EPR spectra (295 K) of cell suspensions (~2 × 10^7 cells in 0.25 mL PBS) in the presence of Cr(VI) (0.50 mM), averages of 20 scans, reaction time 10−20 min. A549-DHA are A549 cells treated with dehydroascorbate (see Table 1 and Experimental Section). Assignments of the signals are shown in Chart 2.

Chart 2. Assignment of EPR Signals[2] for the Reactions of Cr(VI) with Intact Mammalian Cells (Figure 5)

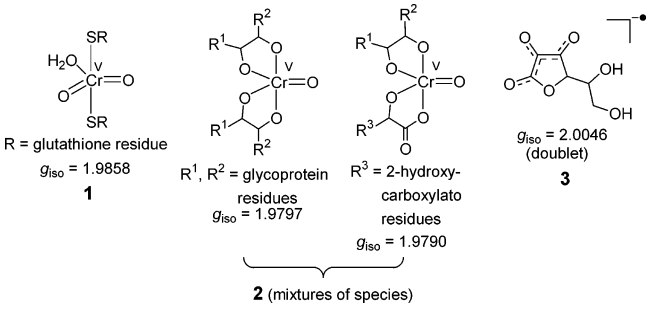

shown in Figure 5, and the assignments of the EPR signals (based on the literature data)[2] are given in Chart 2. No EPR signals were detected in the absence of Cr(VI). For all of the cell lines used (not pretreated with dehydroascorbate), the observed signals were those of Cr(V)-thiolato complexes (g_{iso} = 1.9858, proposed structure **1** in Chart 2, glutathione is the most likely ligand)[89] and those of *O*-donor ligands (carbohydrates and 2-hydroxycarboxylates, g_{iso} = 1.9793−1.9797, **2** in Chart 1).[90] Kinetic studies for the reaction of Cr(VI) with A549 cells (reported elsewhere)[91] showed an increase in relative concentrations of species **2** versus **1** with time (in agreement with the literature data for Cr(VI) reactions with red blood cells).[92] These time-dependent changes are due to ligand-exchange reactions of Cr(V) thiolato complexes, leading to thermodynamically more favorable Cr(V)−carbohydrate complexes.[88−90]

Pretreatment of A549 cells with dehydroascorbate (2.0 mM for 90 min)[65] before the addition of Cr(VI) led to a marked change in the EPR spectra (Figure 5), with the ascorbyl radical (g_{iso} = 2.0046, **3** in Chart 2)[93] becoming a dominant EPR-active species. This change in EPR-active species points to a switch from glutathione to ascorbate as a main Cr(VI) reductant in A549 cells after the pretreatment (which increased the intracellular ascorbate concentration from ~0 to ~1 mM).[65] Notably, this metabolic change did not affect the XANES spectra of Cr(VI)-treated A549 cells (sample **B6** vs **B1a** in Tables 1 and 2 and Figure S6). By contrast, XANES spectra of the Cr(III) products formed during the reactions of Cr(VI) (5.0 mM) with excess glutathione or ascorbate (50 mM) in aqueous solutions (pH 7.0−7.5, adjusted with NaOH, 15 h at 310 K) were

(89) Levina, A.; Zhang, L.; Lay, P. A. *Inorg. Chem.* **2003**, *42*, 767−784.
(90) Codd, R.; Irwin, J. A.; Lay, P. A. *Curr. Opin. Chem. Biol.* **2003**, *7*, 213−219.
(91) Levina, A.; Lay, P. A. *Coord. Chem. Rev.* **2005**, *249*, 281−298.
(92) Sakurai, H.; Takechi, K.; Tsuboi, H.; Yasui, H. *J. Inorg. Biochem.* **1999**, *76*, 71−80.
(93) Laroff, G. P.; Fessenden, R. W.; Schuler, R. H. *J. Am. Chem. Soc.* **1972**, *94*, 9062−9073.

significantly different from each other and from the spectra of Cr(III) in Cr(VI)-treated cells (Figure S6).

Discussion

The results of multiple linear regression analyses of XANES spectra (Table 2 and Figure S8), together with the MS XAFS fittings (Chart 1 and Figures 3b,c and S9), point to amino acid residues (carboxylato, amine, and imidazole) as the most likely donor groups for Cr(III) in Cr(VI)-treated mammalian cells (regardless of the species or organ of origin; samples **B1**−**B9** in Table 1), although smaller amounts of hydroxo or aqua ligands are also likely to be present. These results are consistent with the dominance of *O*-donor ligands in biological Cr(III) complexes, which was suggested based on the comparison of edge energies with those of model complexes (Figure 1). Structures in Chart 1 represent average, rather than unique, coordination environments of Cr(III) in Cr(VI)-treated mammalian cells, although it is likely that they are dominated by one or a few similar environments given the similarity of the spectra from different cell lines. By contrast, oxalato and acetato groups have been suggested as the most likely Cr(III) ligands in Cr(VI)-treated plant cells, based on the analyses of their XANES spectra.[39] The predominant coordination modes of Cr(III) in the animal cell nuclei (containing 10−15% of the total cellular Cr under the studied conditions) are likely to be similar to those in the whole cells, as shown by a close similarity of XANES spectra of samples **B1a**,**b**, **B10**, and **B13** (Table 2 and Supporting Information). A slight difference for sample **B13** is likely to be caused by partial hydrolysis of the Cr complexes during the more lengthy isolation procedure compared with that used for sample **B10** (see Experimental Section). The characteristic XANES spectra of intact Cr(VI)-treated cells were not matched by those for the samples obtained from the in vitro reactions of Cr(VI) or Cr(III) compounds with cell lysate or its fractions (samples **B14**−**B17** in Tables 1 and 2 and Figure S6), which points to the existence of specific metabolic pathways for Cr(VI) in living cells.

Lysis of Cr(VI)-treated A549 cells, followed by separation of the cytoplasmic fraction into HMM and LMM components (∼30 kDa cutoff), leads to a distribution with ∼60% of the total cellular Cr in the LMM fraction (samples **B12a**,**b**). The coordination environment of Cr(III) in **B12a**,**b** is significantly different from that of Cr in intact cells (sample **B1a**,**b**), which is reflected in different XANES and XAFS spectral shapes (Figures 2−4). The regression modeling for the samples **B12a**,**b** implied partial replacement of the amino acid donor groups with aqua ligands (component **A1**, Table 2). These changes are likely to occur due to the hydrolysis of cellular Cr(III) complexes during the lysis and separation procedures, since a combination of XANES spectra of the lysate fractions (**B10**−**B12**, in the proportions corresponding to the relative Cr content in these fractions) could not reproduce the original XANES spectrum of intact cells (Figure S6).

A comparison of XANES spectra of intact Cr(VI)-treated cells and the nucleic, HMM and LMM fractions of their lysate (samples **B1** and **B10**−**B12** in Table 2 and Figures 2 and S6) provides strong evidence that the main part of Cr(III) formed in Cr(VI)-treated cells (including the cytoplasm and the nuclei) is bound to HMM ligands (probably proteins). This analysis is supported by a comparison of XANES and EPR spectroscopic data for the Cr(VI) treatments of ascorbate-deficient and ascorbate-loaded A549 cells (samples **B1** and **B6** in Table 2 and Figure S6). These data show that glutathione and ascorbate (the main Cr(VI) reductants in the respective types of cells) are not the main ligands in the resultant Cr(III) complexes in intact cells, since the change in the type of reductant (evident from the EPR spectra, Figure 5) does not affect the resultant XANES spectra. By contrast, XANES spectra of Cr(III) products obtained from the in vitro Cr(VI) reductions by glutathione or ascorbate were significantly different (Figure S6).

An increase in the proportion of LMM Cr(III) complexes due to the partial hydrolysis of Cr(III)−protein complexes during the subcellular fractionation of Cr(VI)-treated cells reflects a general problem of hydrolysis and redistribution of metal ion complexes during analytical procedures, which greatly complicates the metal speciation studies in biological and environmental samples.[94] Comparison of XANES spectra of metal ions in whole samples with a combination of spectra of separate fractions (taking into account the metal distribution between the fractions) can be used as an efficient diagnostic tool for changes in chemical states of metal ions caused by analytical procedures.

The close similarity between the LMM cytoplasmic fraction of Cr(VI)-treated A549 cells (**B12a**,**b**) and chromodulin (**C**)[11] that was established by comparisons of Cr K-edge XANES and XAFS, and EPR spectroscopies (Figures 2 and 4) is not surprising given that chromodulin has been isolated by size-exclusion and ion-exchange chromatographies as an anionic LMM Cr(III)-containing fraction from the reaction of bovine liver homogenate with Cr(VI).[13] Hence they are expected to be the same species. Moreover, since the Cr K-edge XANES of both the lung A549 cells and the liver HepG2 cells treated with Cr(VI) were very similar, the same species is expected to be isolated using the same procedures from either cell line. Although the chemical nature of Cr(III) in the LMM cellular fraction requires further characterization, it is highly unlikely to consist of a single well-defined Cr(III) complex, as suggested for chromodulin.[11] Chromodulin also does not represent the coordination environment of Cr(III) in intact Cr(VI)-treated mammalian cells (as shown by the comparison of XANES and XAFS data for the samples **B1a,b** and **C** in Figures 2−4). Results of the present work strongly support the previous hypothesis[2,12] that the main source of chromodulin is an artifact of the reported isolation procedure.[13]

Cell treatment conditions used in most of the experiments (0.10 mM Cr(VI) for 4 h at 310 K, Table 1) did not lead to acute toxicity but completely abolished cell propagation (0% clonogenic survival).[18] Slight changes in XANES spectra were observed for the 20-min treatment (sample **B4** in Tables 1 and 2 and Figure S6), which led to ∼100% clonogenic survival of the cells,[18] but these data are more difficult to analyze due to the high noise levels. Future studies will concentrate on the nature of Cr species formed during the prolonged treatments with very low doses of Cr(VI), which are likely to be relevant to the insulin-potentiating effects of Cr(III) compounds.[14,15]

In summary, the results of this study show a great potential of XANES spectroscopy for studies on the biotransformations of exogenous metal ions, such as Cr(VI), in cultured cells.

(94) Sanz-Medel, A.; Soldado Cabezuelo, A. B.; Milačič, R.; Bantan Polak, T. *Coord. Chem. Rev.* **2002**, *228*, 373−383.

Moreover, chromodulin, which is widely thought to be involved in the antidiabetic effects of Cr[11] is likely to be an artifact produced during the reported isolation procedure.[13]

Acknowledgment. Financial support of this work was provided by Australian Research Council (ARC) Discovery Grants and an ARC Professorial Fellowship to P.A.L., an Australian Synchrotron Research Program (ASRP) Postdoctoral Fellowship to H.H.H, an ARC LIEF Grant for the 36-pixel Ge detector at ANBF, and a Wellcome Trust and ARC grants for the EPR equipment. X-ray absorption spectroscopy was performed partially at ANBF with support from ASRP, which is funded by the Commonwealth of Australia under the Major National Research Facilities program, and partially at SSRL, which is operated by the Department of Energy, Office of Basic Energy Sciences. The SSRL Biotechnology Program is supported by the National Institutes of Health, National Center for Research Resources, Biomedical Technology Program, and by the Department of Energy, Office of Biological and Environmental Research. We thank Drs. Garry Foran and Matthew Latimer for the assistance with XAS experiments at ANBF and SSRL, respectively, and Dr. Henrietta Headlam and Ms. Irma Mulyani (The University of Sydney) for the syntheses of some of the model Cr(III) compounds.

Supporting Information Available: Synthesis and characterization (including circular dichroism and XANES spectra) of model Cr(III) complexes, representative optical micrographs indicating typical morphologies of cell lines, comparisons of cell-derived and model Cr(III) XANES spectra; principal component analysis of XANES of Cr(III) in biological samples, and details MS XAFS analyses. This material is available free of charge via the Internet at http://pubs.acs.org.

JA063792R